bioresources.com

Dimensional Behavior of Nail-Laminated Timber-Concrete Composite Caused by Changes in Ambient Air, and Correlation among Temperature, Relative Humidity, and Strain

Sung-Wook Hwang,[a] Hyunwoo Chung,[b] Taekyeong Lee,[a] Kyung-Sun Ahn,[c] Sung-Jun Pang,[a] Ji Yong Kim,[c] Junsik Bang,[c] Minjung Jung,[c] Jung-Kwon Oh,[a,b,c] Hyo Won Kwak,[a,b,c] and Hwanmyeong Yeo [a,b,c,]*

A timber-concrete composite (TCC) slab composed of nail-laminated timber (NLT) and topping concrete (TC) was developed for flooring applications. The NLT was laminated alternately with lumber and plywood. To investigate the dimensional behavior of the TCC slab, the temperature, relative humidity (RH), and dimensional changes of the slab exposed to outdoor air were monitored for 205 days. Temperature change was directly transmitted to both components, and RH change was gradually transmitted to the NLT. Concrete pouring caused a sharp increase in NLT width, which was the laminating direction of the nails. This resulted from swelling of the wood because of the moisture in the concrete mixture and loosening of the nail lamination. The member composition for the nail-laminating system, fastener type, and concrete volume help to secure the dimensional stability of the NLT. Cracks in the TC caused width deformation, which was recovered by drying shrinkage of the TC. Correlation analysis among temperature, RH, and strain indicated that dimensional changes in NLT correlated strongly with RH, while those in TC correlated strongly with temperature. The correlation between longitudinal strain in the TC and strain in the three directions of the NLT was attributed to the notches designed for mechanical connection.

INTRODUCTION

Mass timber, the fruit of the advancement of engineered wood, is a large-scale structural material formed by laminating dimension lumber with adhesives, nails, and dowels. Cross-laminated timber (CLT), dowel-laminated timber (DLT), glued-laminated timber (GLT), and nail-laminated timber (NLT) are representative mass timber products. Mass timber construction has turned wood, a material for small buildings, into a structural material suitable for large buildings, and a competitor for steel and concrete (Abed *et al*.

2022). Replacing steel and concrete with mass timber products reduces the potential for global warming by 18.0 to 26.5%, even without considering the carbon fixed in the wood itself (Pierobon *et al.* 2019; Liang *et al.* 2020). Hence, the use of mass timber products as sustainable materials can be a practical solution for achieving low carbon emission and energy efficiency.

The manufacture of NLT requires only the most basic building materials and tools, such as wood and nails. The ease of fabrication of NLT panels has made them useful as walls, elevator and stair shafts, shear walls, and roofs for more than a century (Binational Softwood Lumber Council 2017; Hong 2017). The emergence of environmental issues caused by global warming is now creating new opportunities for mass timber, such as NLT. A nail-laminated timber-concrete composite (TCC) is a structural system that integrates wood and concrete, maximizing the inherent strengths of concrete and wood, and complementing their shortcomings (Yeoh 2010; Hong 2017). Numerous studies on the structural performance and behavior of NLT and TCC have been reported (Lukaszewska *et al.* 2008; Yeoh *et al.* 2011; Fragiacomo *et al.* 2018; Derikvand *et al.* 2019; Pang *et al.* 2022). However, the behavior due to moisture changes was not the primary concern of these studies.

Wood, a hygroscopic material, undergoes repeated moisture absorption and desorption depending on the surrounding climate, and this causes dimensional changes. A continuous high-humidity environment and the resulting high moisture content of wood can threaten structural stability by causing deterioration of wood strength, biological damage, and swelling (Franke *et al.* 2015; Dietsch and Winter 2018; Bobadilha *et al.* 2020; Sinha *et al.* 2020). Therefore, precise moisture determination is essential for wooden materials, and long-term observations of moisture and dimensional changes are required for structures using mass timber products.

Electrical resistance-based methods are standard approaches for moisture determination in wood used in large structures (Brischke *et al.* 2008; Dietsch *et al.* 2015; Björngrim *et al.* 2016; Hwang *et al.* 2021). However, electrical methods must control factors such as wood species, internal stress, preservatives, the position and distance of the inserted electrodes, and incomplete electrode contact (Hwang *et al.* 2021). High-frequency and near-infrared spectroscopy measurements, another approach for moisture determination, must consider the high cost and stability of long-term field observations. A hygrometric method that determines moisture content using wood properties in equilibrium with the surrounding climate can be a good alternative. The equilibrium moisture content (EMC) can be calculated from the temperature and relative humidity (RH) of the enclosed space inside wood using the sorption equation (Hailwood and Horrobin 1946). This method has fewer limitations in terms of internal moisture measurements and long-term observation.

Through long-term observation of a TCC slab developed for flooring applications, this study describes the moisture fluctuation and the resulting dimensional behavior of NLT and concrete, which are elements of the TCC slab. Long-term monitoring of the moisture and dimensional behavior of NLT panels has been reported (Hwang *et al.* 2022), but the composite behavior of NLT and concrete has yet to be investigated. To the best of our knowledge, this is the first report on the correlation between NLT and concrete for the dimensional behavior of TCC systems. The findings of this study can be used as primary data for TCC-based structure design and structural safety evaluation.

EXPERIMENTAL

NLT-Concrete Composite Slab

NLT panel

A TCC slab for observing moisture and dimensional changes was designed with an underlying NLT panel connected to a concrete slab. As shown in Fig. 1, the NLT consists of 24 mm × 140 mm × 2000 mm (radial × tangential × longitudinal directions) lumber and 24 mm × 245 mm × 2000 mm (thickness × height × length) 9-ply plywood. All lumber was flat sawn wood. The wood species used for lumber and plywood was Japanese larch (*Larix kaempferi*). A total of 42 elements, 21 each of lumber and plywood, were used to fabricate the NLT. The lumber and plywood were alternately fastened with nails with head diameter, shank diameter, and length of 7 mm, 2.9 mm, and 75 mm, respectively. The end distance, edge distance, and spacing of nails for lamination nailing were 45, 25, and 120 mm, respectively. The end distance and edge distance were determined by EN 1995-1-1 (2004), and the spacing of the nails followed the recommendations of the Nail-laminated Timber U. S. Design & Construction Guide (Binational Softwood Lumber Council 2017). The air-dry densities of the lumber and plywood were 0.55 and 0.66 g/cm^3, respectively. Plywood higher than the lumber formed bulkheads on the upper surface of the NLT. Additionally, the plywood had five notches with a height of 35 mm, length of 15 mm, and edge angle of 90° at the center, spaced 90 mm apart, to improve the slip modulus.
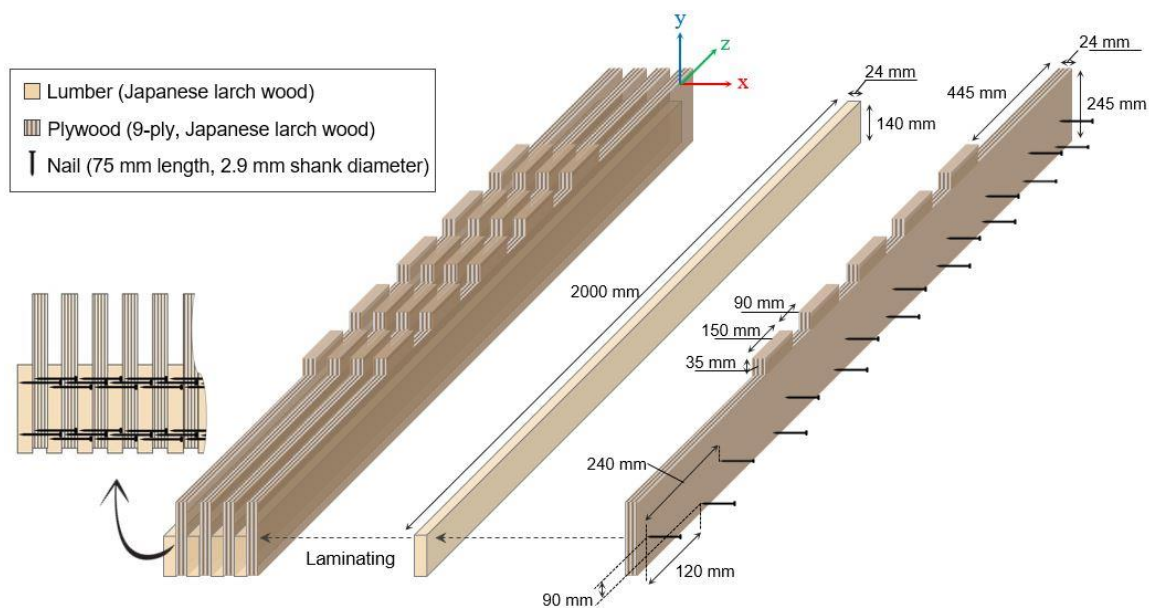

Fig. 1. Elements and lamination schemes of the nail-laminated timber panel used to fabricate the slab specimen

Topping concrete

Topping concrete (TC) was formed by pouring ready-mixed concrete composed of Portland cement onto the NLT with a 1000 mm × 200 mm × 2000 mm (width × height × length) mold. The nominal strength, the nominal maximum size of the coarse aggregate, and the slump flow of the concrete mixture were 24 MPa, 25 mm, and 120 mm, respectively. The TC was 185-mm-thick based on the height of the underlying lumber and 80-mm-thick

based on the height of the plywood, not including the notch height. The wet concrete was cured while exposed to ambient conditions. Finally, a TCC slab with dimensions of 1000 mm (width, X-direction) × 320 mm (height, Y-direction) × 2000 mm (length, Z-direction) was manufactured (Fig. 2a) and used to observe moisture and dimensional changes.
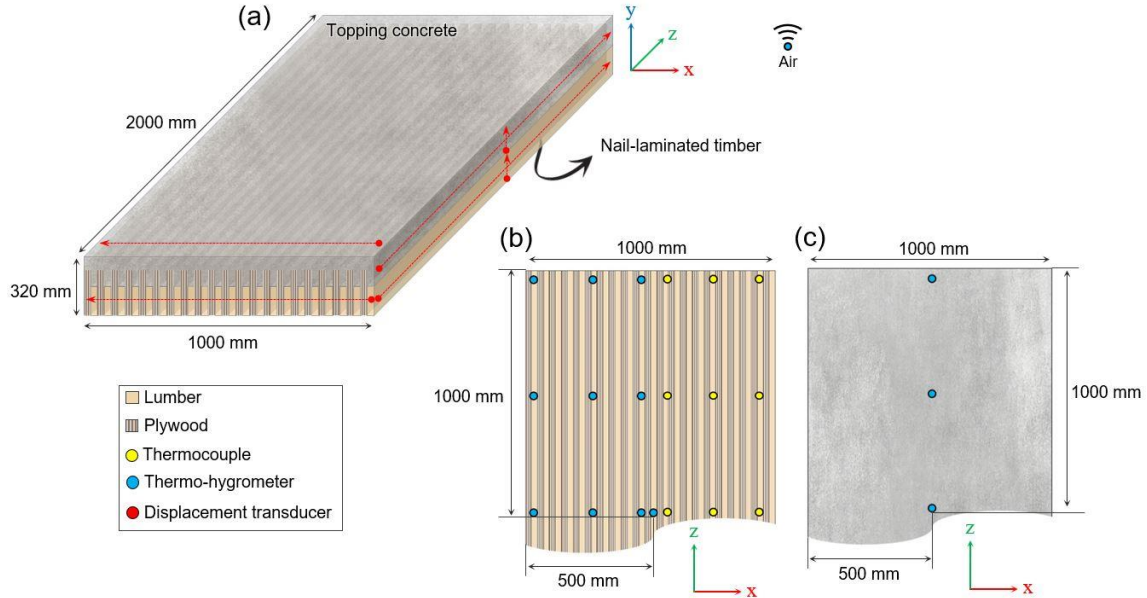
Fig. 2. Configuration of the slab specimen and installed sensors for observation: (a) Nail-laminated timber-concrete composite, (b) nail-laminated timber, and (c) topping concrete

Observation Details

Observation site and period

The TCC slab was placed outdoors on the Seoul National University campus to investigate the dimensional behavior of the slab resulting from fluctuations in the outdoor air. A canopy was built over the slab to prevent direct contact with sunlight and rain. Because the observation site (37°45'79.03" N, 126°94'79.62" E) was located near forests and streams, the RH of the site was somewhat higher than that of the reference point in Seoul (Hwang *et al.* 2022). The climatic conditions of the observation site are harsher than those where TCC is typically used.

Table 1. Details for Observation of Moisture and Dimensional Behavior of the TCC Slab

Element	Measurement	Period (YY/MM/DD)	Sensor (Quantity)	Position
Air	Temp. & RH	22/03/07 to 22/09/27	Thermo-hygrometer (1)	Outdoor
NLT	Temp.	22/03/07 to 22/09/27	Thermocouple (9)	Inside
	Temp. & RH	22/03/07 to 22/09/27	Thermo-hygrometer (10)	Inside
	Strain	22/05/05 to 22/09/27	Displacement transducer (3)	Surface
TC	Temp. & RH	22/05/30 to 22/09/27	Thermo-hygrometer (3)	Inside
	Strain	22/06/15 to 22/09/27	Displacement transducer (3)	Surface

This study dealt with temperature, RH, and dimensional data collected from March 7 to September 27, 2022 (205 days) for a TCC slab. Because the concrete was poured (May 30, 2022) and cured during the observation period, the observation period for each element of the TCC slab was different, as listed in Table 1.

Sensors

The sensors used to observe the temperature, RH, and dimensional changes in the TCC slab are listed in Table 1. A probe-type thermo-hygrometer (HMP 60, Vaisala, Vantaa, Finland) was placed in an instrument shelter in the canopy to measure the temperature and RH of the air.

Nine K-type thermocouples were installed inside the lumber elements in the bottom quadrant to measure the temperature of the NLT, as shown in Fig. 2b. Meanwhile, nine coin-type thermo-hygrometers (DS 1923, Maxim Integrated, San Jose, CA, USA) for measuring temperature and RH were installed at points opposite to where the thermocouples were installed. All DS 1923 sensors used in this study were sealed with a waterproof/breathable fabric made of expanded polytetrafluoroethylene (ePTFE), known as Gore-Tex, to prevent moisture ingress into the sensor. In addition, a thermo-hygrometer (HMP60) was installed at the center of the NLT as a spare. All thermocouples and thermo-hygrometers were placed at a depth of 7 cm in the middle of the lumber height. The holes where the sensors were located were double-sealed with a polyvinyl acetate adhesive and silicone sealant to prevent the inflow of ambient air.

Three thermo-hygrometers (DS1923) were installed inside the concrete layer to measure the temperature and relative humidity (RH) of the TC (Fig. 2c). It is difficult to accurately position the sensors in the middle of the TC height during concrete pouring. Hence, concrete bars with dimensions of 24 mm × 180 mm × 24 mm (width × height × length) were prefabricated with an ePTFE-sealed sensor positioned at the center of the bar. Concrete bars were placed on the central lumber of the NLT, and concrete was poured over them.

Wire tension-type displacement transducers (DP-500G, Tokyo Measuring Instruments Laboratory, Tokyo, Japan) were used to measure dimensional changes in the TCC slab elements. Dimensional changes in the width (X), height (Y), and length (Z) of the elements were determined using six displacement transducers installed on the surfaces of the NLT and TC.

Data acquisition

All sensors were monitored by a data logger (CR1000, Campbell Scientific, Logan, UT, USA) equipped with a relay multiplexer (AM16/32B, Campbell Scientific), except for the DS 1923 thermo-hygrometer with a built-in data logger. The DS 1923 sensors stored the temperature and RH at 1-h intervals. The other sensors recorded measurements at 30-s intervals, and the data logger stored 1-h and 24-h average measurements. The dedicated software of the data logger provided data management and real-time monitoring.

Evaluation of Changes in Moisture and Dimension
EMC

To evaluate the moisture in the NLT, the temperature and RH data acquired from the thermo-hygrometers were converted into EMC using Eq. 1 (Glass and Zelinka 2010) based on the Hailwood–Horrobin sorption model (Hailwood and Horrobin 1946),

$$\text{EMC} = \frac{1800}{W}\left(\frac{kh}{1-kh} + \frac{k_1 kh + 2k_1 k_2 k^2 h^2}{1 + k_1 kh + k_1 k_2 k^2 h^2}\right) \tag{1}$$

$$W = 349 + 1.29T + 0.0135T^2$$

$$k = 0.805 + 0.000736T + 0.00000273T^2$$

$$k_1 = 6.27 - 0.00938T - 0.000303T^2$$

$$k_2 = 1.91 + 0.0407T - 0.000293T^2$$

where h is the RH (%); T is the temperature (°C); and W, k, k_1, and k_2 are variables related to temperature. Plywood is known to have a slightly lower EMC than solid wood (APA 2010), but the difference decreases as RH increases. Hence, this study assumed that the EMC of both components was similar.

Strain

The measurements in the three orthogonal directions obtained from the displacement transducers were converted to strain using Eq. 2 to evaluate dimensional changes in the TCC elements,

$$\varepsilon = \frac{l_d - l_i}{l_i} \times 100 \ (\%), \tag{2}$$

where ε is the linear strain in a single direction, and l_i and l_d are the initial and deformed lengths, respectively.

Correlation Analysis

The Pearson correlation coefficient was used to quantify the relationship between the variables related to moisture and the dimensional behavior of TCC elements. The correlation coefficient indicating a linear relationship between the two variables was calculated using Eq. 3,

$$r = \frac{n\sum ab - (\sum a)(\sum b)}{\sqrt{\left[n\sum a^2 - (\sum a)^2\right]\left[n\sum b^2 - (\sum b)^2\right]}}, \tag{3}$$

where r is the correlation coefficient, n is the sample size, and a and b are the observations of the two variables.

The Student's t-test was performed using Python 3.8 with the open-source library SciPy to determine whether the relationship between the variables was significant. The t-score was calculated from the correlation coefficient using Eq. 4, and the significance of the association was evaluated with significance levels of 0.05 and 0.01 for the two-tailed p-value.

$$t = \frac{r}{\sqrt{(1-r^2)/(n-2)}}, \tag{4}$$

RESULTS AND DISCUSSION

Temperature and RH Changes
NLT panel

Figure 3 shows the temperature changes at nine points inside the NLT and in the air. Initially, the NLT temperatures were lower than the air temperature. After the air temperature increased to approximately 15 °C, the NLT and air temperatures remained at a similar level. Fluctuations in the air temperature were directly transferred into the NLT. The inset in Fig. 3 shows that the temperatures of the NLT at nine points fluctuated by forming two clusters. The two clusters correspond to different sensor positions, that is, the edges and center of the NLT. This indicates that the temperature transfer rate differed for each part of the NLT. The temperature difference inside the NLT was monitored throughout the observation period, including when the concrete was poured. Descriptive statistics of the air and NLT temperature data are presented in Table 2.
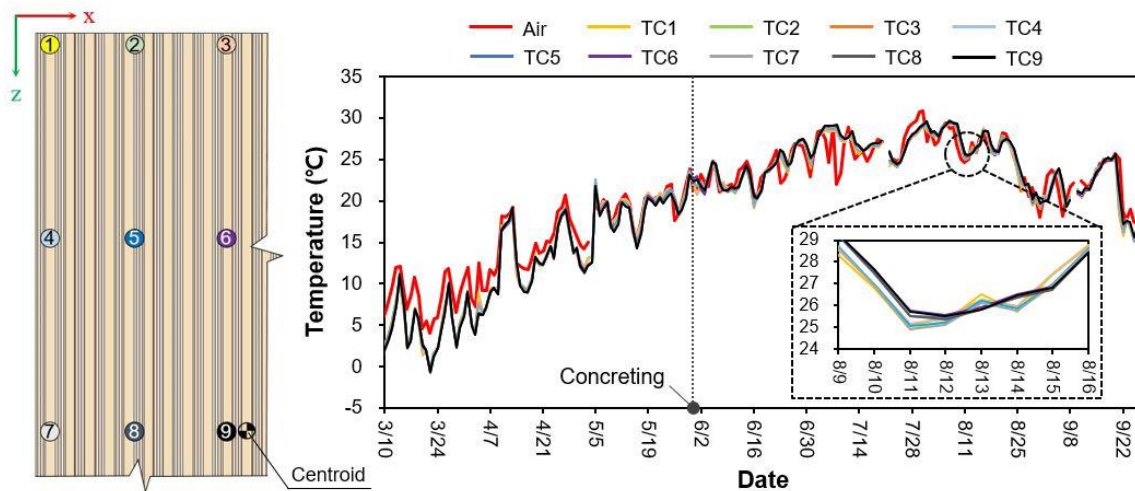

Fig. 3. Changes in temperature of ambient air and inside nail-laminated timber

Table 2. Descriptive Statistics of Temperature, RH, and EMC Acquired from Elements of the TCC Slab and Ambient Air

Element	Measurement	N	Min	Max	Range	Mean	SD
Air	Temp. (°C)	205	1.9	30.9	29.0	20.2	6.4
	RH (%)	205	29.9	91.9	62.0	70.9	13.5
	EMC (%)	205	6.0	23.1	17.1	14.0	3.7
NLT	Temp. (°C)	205	-2.7	29.5	32.2	19.2	8.0
	RH (%)	205	45.4	79.1	33.7	65.3	11.0
	EMC (%)	205	9.3	16.3	7.0	12.7	2.4
TC	Temp. (°C)	120	17.4	29.0	11.7	24.8	2.9
	RH	120	92.5	100.0	7.5	96.9	2.8

Notes: N, number of observations; Min, minimum; Max, maximum; SD, standard deviation

In contrast to the temperature change, the noticeable fluctuation in the RH of the air was transmitted gently into the NLT because of the humidification effect of the wood (Fig. 4a). However, the variation pattern of RH could be divided into two clusters, similar to the behavior of the temperature. In the early stages of observation, the RH values of the sensors located at the edges were higher than those of the central sensors. However, this behavior was reversed when the concrete was poured. Within 24 h after concreting, the RH of sensor no. 9, closest to the centroid of the NLT, increased from 55.9% to 62.0%, and after a week, the value increased to 67.2%. This sharp increase was observed in the sensors at the center but not at the edge. The RH change at the edge seemed to be dominated by air RH rather than moisture introduced by the concrete.
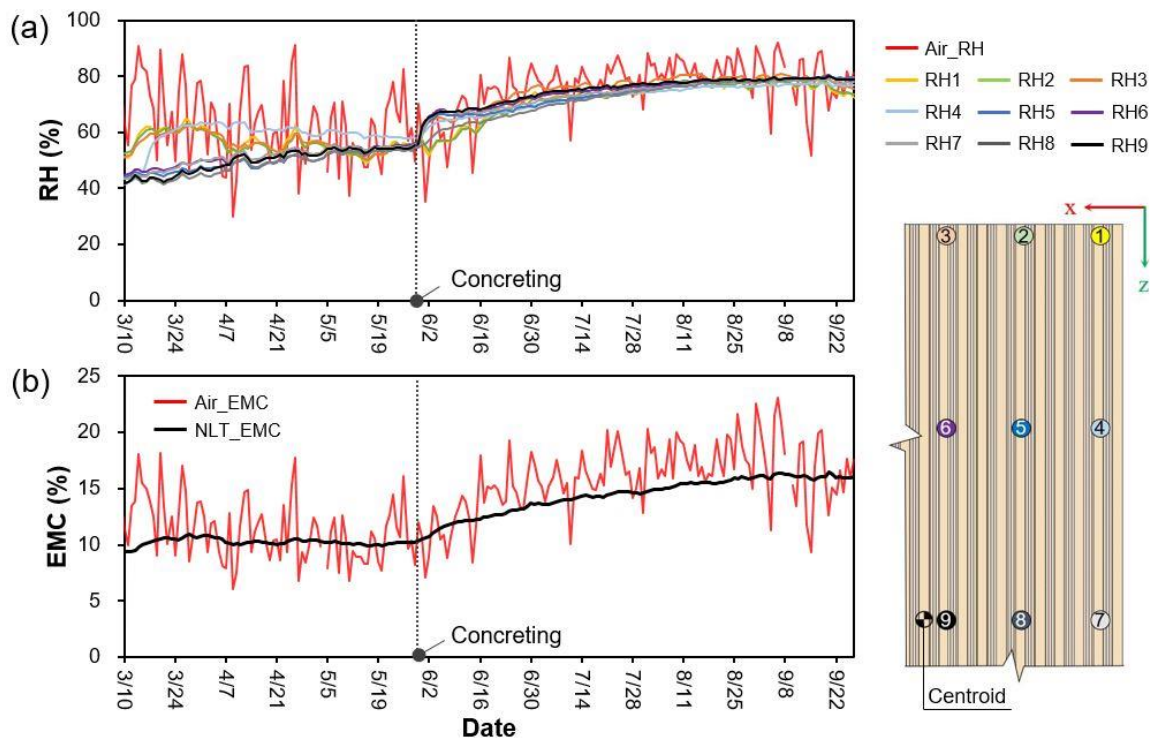

Fig. 4. Changes in relative humidity (a) and equilibrium moisture content (b) at nine measuring points inside nail-laminated timber

The EMC of the NLT and air calculated from the temperature and RH are depicted in Fig. 4b. The EMC is the average of nine measurements. The humid climate in the summer increased the air EMC, which caused an increase in the EMC of the NLT. The EMC of the NLT started at a low level of 9.3% on the first day of observation and peaked at 16.3% on September 5 (Table 2). The minimum and maximum values at the center were 8.7% and 16.7%, respectively. The EMCs are within a safe range for strength degradation and biodegradation (Shupe *et al.* 2008; Kirker *et al.* 2016). Concrete pouring caused an increase in the EMC of the NLT. A week after concreting, the EMC had increased 1.5% from 10.3% to 11.8%. Since then, the EMC continued to grow, influenced by a large amount of water in the concrete and an increasing ambient RH. Although the increase in EMC by concreting did not threaten the safety of the NLT, it is worth considering the formation of a moisture barrier using waterproof paint to minimize the increase in internal moisture (Fragiacomo *et al.* 2018; Ou *et al.* 2020).

Topping concrete

Figure 5 shows the temperature and RH trends in the TC. Similar to NLT, temperature fluctuations in the air were reflected inside the TC. Although not exceptionally high, a temperature slightly higher than that of air was seen in the TC at the beginning of curing, which was likely because of the heat of hydration of concrete (Kaleta-Jurowska and Jurowski 2020). The internal RH of the TC during curing was maintained at 100% and then decreased from the edge after 15 d, and from the center after a month. Temperature variation is a factor that induces the thermal expansion or contraction of concrete (Ng and Kwan 2016), and a decrease in RH during curing, *i.e.*, evaporation of free water, can lead to drying shrinkage (Sakata 1983). Displacement transducers captured the deformation of the TC because of temperature and RH fluctuations.
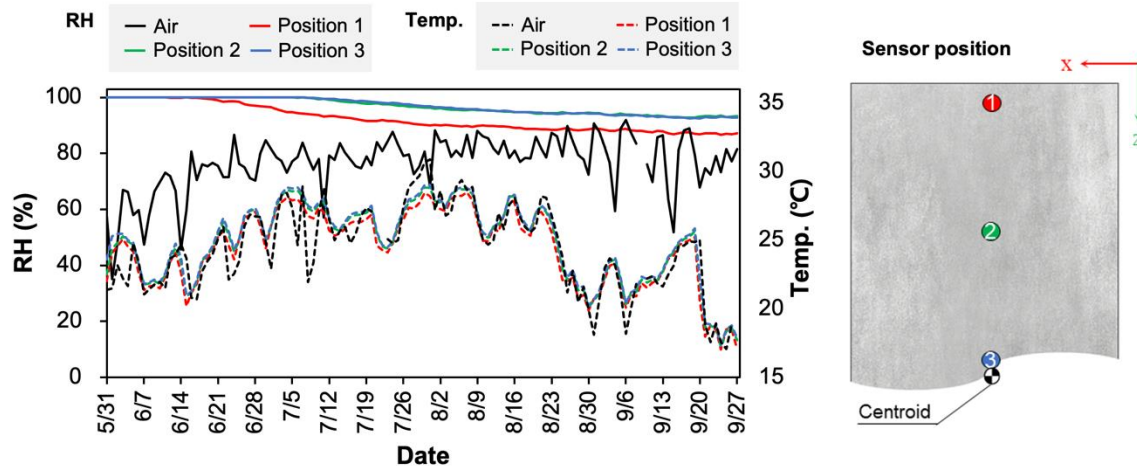
Fig. 5. Temperature and relative humidity changes in topping concrete

Dimensional Changes

NLT panel

The NLT strain in three directions *versus* time is plotted in Fig. 6a. The strain in the height (Y-direction) corresponding to the tangential direction of the wood was the highest, followed by that in the width (X-direction) corresponding to the radial direction. The maximum strain in each direction was 1.46% and 0.80%, respectively (Table 3).

Table 3. Descriptive Statistics for Strains of Elements of the TCC Slab

Element	Structural Direction	N	Min	Max	Range	Mean	SD
NLT	Width (X)	146	-0.10	0.80	0.91	0.54	0.29
	Height (Y)	146	-0.41	1.46	1.87	0.67	0.54
	Length (Z)	146	-0.02	0.02	0.05	0.01	0.01
TC	Width (X)	105	-0.20	1.72	1.92	0.83	0.66
	Height (Y)	105	-0.04	0.16	0.20	0.08	0.04
	Length (Z)	105	-0.03	0.05	0.08	0.02	0.02

Notes: N, number of observations; Min, minimum; Max, maximum; SD, standard deviation

bioresources.com

The longitudinal (Z-direction) strain was negligible with a maximum value of 0.02%. The normalized strain in the three directions shows a pattern resembling the internal RH fluctuations of the NLT (Fig. 6b), indicating that moisture fluctuations induce dimensional changes.
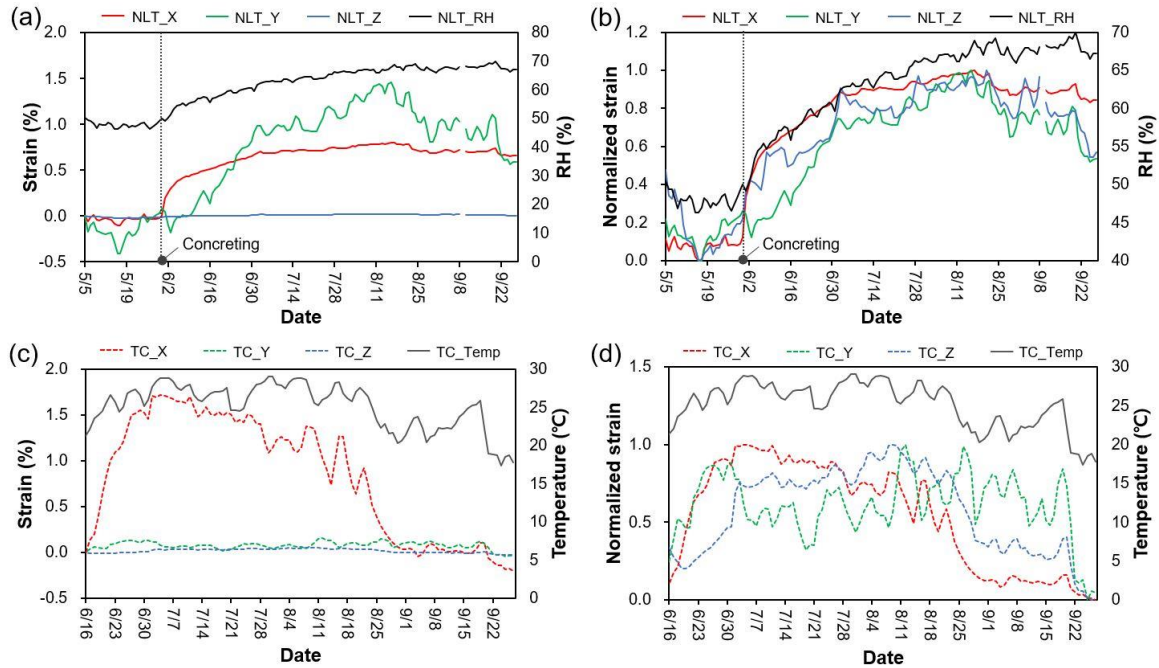
Fig. 6. Original and normalized strain in three orthogonal directions of nail-laminated timber (a, b) and topping concrete (c, d)

Concrete pouring resulted in a sharp increase in width. The nature of the NLT system, in which nails mechanically fasten the elements in the X-direction, suggests relatively weak dimensional stability in this direction (Binational Softwood Lumber Council 2017). In other words, the sharp increase after concreting indicates that the nail-laminated structure loosened because of the load and moisture of the concrete (Fig. 7).

Fig. 7. The space created between the lamination of nail-laminated timber by concrete pouring

One week after concreting, the width strain increased from 0.1% to 0.43%, corresponding to a strain of 0.28% per 1% EMC. Because the reported shrinkages per 1% MC in the radial direction of Japanese larch lumber and plywood are approximately 0.142% (Kim and Lee 2002; Park *et al.* 2015) and 0.126% (Hwang *et al.* 2022), respectively, it is considered that the moisture and concrete load contributes similarly to the width swelling.

The RH continuously rose, starting in mid-June, and the strain in the X-direction and its fluctuation range were smaller than those in the Y-direction (Fig. 6a). This can be explained by the swelling anisotropy of wood. Another factor to be considered in interpreting the phenomenon is that the gap between the elements caused by the rapid increase in width after concreting offsets the actual swelling of the elements in the X-direction.

Hwang *et al.* (2022) reported that the width strain of an NLT with a flat surface increased 0.23% after concreting. In addition, they stated that the moisture inside the NLT was not significantly affected by concreting and that the load of the concrete dominated the rapid width increase. The width strain observed in this study was higher than the values reported by Hwang *et al*. The higher strain is a result of a combination of the following three factors:

(1) Higher concrete volume: The volume of concrete poured per square meter of NLT surface area was 0.122 m^3, which is approximately 22% higher. The higher concrete load applied to the NLT results in further loosening of the nail-laminated structure.

(2) Bulkhead structure of NLT: Concrete pouring applies a flexural load to the NLT, resulting in width deformation. However, the bulkheads of the plywood elements accelerate this deformation because they create an additional moment.

(3) Fasteners: This study used nails to fasten the elements, whereas screws were used in the Hwang study. The withdrawal resistance force of the nails and screws used, calculated according to EN 1995-1-1 (2004) are approximately 1500 N and 16,000 N, respectively, indicating that the screws were more than ten times stronger. Fasteners are an essential factor in mechanical bonding between members. Thus, nailed lamination resulted in a more significant deformation than screwed lamination.

Therefore, the width strain of the NLT in this study was greater than the value reported by Hwang. Additionally, the wider gap between the elements created by width swelling may have contributed to the increase in internal moisture. The width swelling immediately after concreting is a permanent deformation that does not recover, even if the RH of the air is sufficiently low (Hwang *et al.* 2022).

Topping concrete

Dimensional changes in the TC were recorded by installing displacement transducers two weeks after concreting. The deformation of the TC was based on its width (Fig. 6c). At an early stage, the strain in the X-direction increased rapidly to a maximum of 1.72%, and then it continuously decreased. Meanwhile, the maximum strain in the Y- and Z-directions was only 0.16% and 0.05%, respectively (Table 3).

Considering that concrete is an isotropic material, remarkable deformation in the X-direction is unusual. Several surface cracks that developed during curing were observed. Cracks can occur because of a thermal gap between the inside and outside of the structure

and rapid water loss during curing (Holt and Leivo 2004; Ha *et al.* 2014). In this study, hairline cracks were observed on the surface of the TC. Additionally, the gap widened, while the internal RH of the TC was maintained at 100%, because of the difference in dryness between the surface and center. These factors likely affected the increase in width. The width recovery was attributed to drying shrinkage, as a decrease in the X-direction strain and a decrease in the internal RH to less than 100% coincided. The decrease in the strain of NLT in the three directions observed during the rising phase of RH at the end of the observation may suggest partial composite behavior of TCC due to the drying shrinkage of TC.

Although the strain in the Y-direction deviated from the pattern in some sections, the variation pattern of the normalized strain plots in the three directions resembles that of the TC temperature (Fig. 6d). These results indicate that the temperature is a factor in the dimensional change of concrete.

Correlation Analysis

Correlation coefficients (r) were calculated to determine the relationships between TCC slab parameters (Fig. 8). The internal RH of the NLT showed the strongest correlation with the dimensional change in the NLT. The correlations between RH and strain of the NLT were very strong for the X-direction (r = 0.94), strong for the Y-direction (r = 0.74), and moderate for the Z-direction (r = 0.65). The correlations were considered statistically significant at p < 0.01.
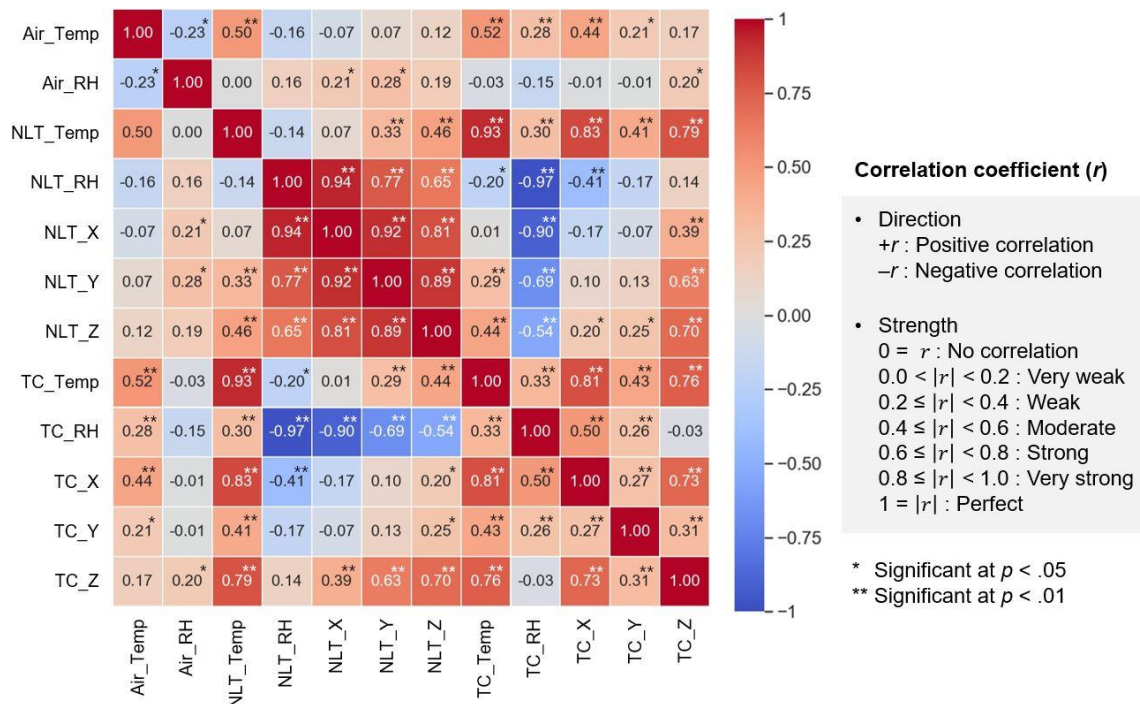
Fig. 8. Heatmap showing correlation coefficients between parameters of data acquired

Although not as strong as the correlation between RH and strain of the NLT, the temperature was strongly associated with the dimensional change of the TC. The strain in the X- and Z-directions of the TC was strongly correlated with the temperature with

statistical significance. The X strain and RH of the TC were moderately correlated, with r = 0.5 and p < 0.01, indicating that the width recovery (Fig. 6c) of the TC was a result of drying shrinkage represented by the decrease in RH (Fig. 5). The strain in the Y-direction behaved independently compared with the other directions.

The correlation of the strain between the NLT and TC showed different aspects in each direction. The strain in the X- and Y-directions of the TC was weakly correlated with the strain in the three directions of the NLT. In contrast, the strain of the TC in the Z-direction was strongly correlated with the strain of the NLT in the Y- and Z-directions, with statistical significance. This strong correlation is likely because the notches in the plywood of the NLT act as transmitters to transfer the deformation of the TC to the NLT and *vice versa*. Similarly, the bulkheads formed by the plywood are expected to be transmitters in the X-direction. However, there was no correlation between the X-directions of the NLT and the TC. This result is attributed to the occurrence of surface cracks and incomplete concrete curing. Deformation of the TC in the X-direction was dominated by cracks that developed and an internal RH that did not reach a constant, so it is not easy to find a correlation between deformations in the X-direction of the NLT and the TC. This issue will be investigated through additional data acquisition and analyses. The Y-direction strain of the TC, which exhibited independent behavior, showed a very weak correlation with the strain in other directions, except for the strain in the Z-direction of the NLT, which was weakly correlated but not statistically significant.

Correlation analysis suggested that the key parameters affecting the dimensional behavior of NLT and TC were RH and temperature, respectively, and provided clues to the partial composite behavior between NLT and TC. Observation of the TCC slabs is ongoing, and data are still accumulating. Further investigations will report the results regarding the long-term dimensional behavior of the TCC slab.

CONCLUSIONS

1. The temperature changes in the nail-laminated timber (NLT) and topping concrete (TC) directly reflected temperature fluctuations in the air. In contrast, relative humidity (RH) changes in the air were transferred gradually into the NLT. Temperature and RH changes in the NLT differed between the edge and center.

2. Concrete pouring increased the moisture and dimensionality of the NLT. A week after concreting, the equilibrium moisture content (EMC) and width strain increased by 1.5% and 0.42%, respectively. The width deformation was likely caused by a combination of the expansion of wood and plywood elements due to a large amount of moisture in wet concrete and the loosening of the nail lamination system due to concrete load.

3. Surface cracks in the TC developed at the beginning of the concrete curing were the likely cause of significant deformation in width. The width deformation recovered with a decrease in the internal RH, suggesting drying shrinkage of the concrete. The dimensional change in the TC followed the temperature fluctuation rather than that of the RH.

4. The parameters highly correlated with dimensional changes in NLT and TC were RH and temperature, respectively. The strain in the three dimensions of the NLT was strongly correlated with each other, while the change in the height of the TC was relatively independent.

To specify the effect of concrete load on the width increase of NLT after concrete pouring, it is necessary to investigate the dimensional behavior of NLT with waterproof paint applied. In addition, the strength of TCC slabs before and after exposure to outdoor conditions is essential information for structural stability. These lines of investigation are in progress and will be reported elsewhere.

ACKNOWLEDGEMENTS

REFERENCES CITED

APA (2010). "Technical topics: Moisture-related dimensional stability," APA – The Engineered Wood Association, Tacoma, WA, USA.

Abed, J., Rayburg, S., Rodwell, J., and Neave, M. (2022). "A review of the performance and benefits of mass timber as an alternative to concrete and steel for improving the sustainability of structures," *Sustainability* 14(9), article 5570. DOI: 10.3390/su14095570

Binational Softwood Lumber Council (2017). *Nail-laminated Timber U. S. Design & Construction Guide v1.0*, Binational Softwood Lumber Council, Surrey, BC, Canada.

Bobadilha, G. S., Stokes, C. E., Kirker, G., Ahmed, S. A., Ohno, K. M., and Lopes, D. J. V. (2020). "Effect of exterior wood coatings on the durability of cross-laminated timber against mold and decay fungi," *BioResources* 15(4), 8420-8433. DOI: 10.15376/biores.15.4.8420-8433

Björngrim, N., Hagman, O., and Wang, X. A. (2016). "Moisture content monitoring of a timber footbridge," *BioResources* 11(2), 3904-3913. DOI: 10.15376/biores.11.2.3904-3913

Brischke, C., Rapp, A. O., and Bayerbach, R. (2008). "Measurement system for long-term recording of wood moisture content with internal conductively glued electrodes," *Building and Environment* 43(10), 1566-1574. DOI: 10.1016/j.buildenv.2007.10.002

Derikvand, M., Jiao, H., Kotlarewski, N., Lee, M., Chan, A., and Nolan, G. (2019). "Bending performance of nail-laminated timber constructed of fast-grown plantation eucalypt," *European Journal of Wood and Wood Products* 77(3), 421-437. DOI: 10.1007/s00107-019-01408-9

Dietsch, P., Franke, S., Franke, B., Gamper, A., and Winter, S. (2015). "Methods to determine wood moisture content and their applicability in monitoring concepts,"

Journal of Civil Structural Health Monitoring 5(2), 115-127. DOI: 10.1007/s13349-014-0082-7

Dietsch, P., and Winter, S. (2018). "Structural failure in large- span timber structures: A comprehensive analysis of 230 cases," *Structural Safety* 71, 41-46. DOI: 10.1016/j.strusafe.2017.11.004

EN 1995-1-1 (2004). "Eurocode 5: Design of timber structures - Part 1-1: General - Common rules and rules for buildings," European Committee for Standardization, Brussels, Belgium.

Fragiacomo, M., Gregori, A., Xue, J., Demartino, C., and Toso, M. (2018). "Timber-concrete composite bridges: Three case studies," *Journal of Traffic and Transportation Engineering* 5(6), 429-438. DOI: 10.1016/j.jtte.2018.09.001

Franke, B., Franke, S., and Müller, A. (2015). "Case studies: Long-term monitoring of timber bridges," *Journal of Civil Structural Health Monitoring* 5(2), 195-202. DOI: 10.1007/s13349-014-0093-4

Glass, S. V., and Zelinka, S. L. (2010). "Moisture relations and physical properties of wood," in: *Wood Handbook: Wood as an Engineering Material*, Forest Products Laboratory, Forest Service, United States Department of Agriculture, Madison, WI, USA, pp. 1-19.

Ha, J. H., Jung, Y. S., and Cho, Y. G. (2014). "Thermal crack control in mass concrete structure using an automated curing system," *Automation in Construction* 45, 16-24. DOI: 10.1016/j.autcon.2014.04.014

Hailwood, A. J., and Horrobin, S. (1946). "Absorption of water by polymers: Analysis in terms of a simple model," *Transactions of the Faraday Society* 42, B084-B092.

Holt, E., and Leivo, M. (2004). "Cracking risks associated with early age shrinkage," *Cement and Concrete Composites* 26(5), 521-530. DOI: 10.1016/S0958-9465(03)00068-4

Hong, K. E. M. (2017). *Structural Performance of Nail-Laminated Timber-Concrete Composite Floors*, Doctoral Thesis, University of British Columbia, Vancouver, Canada.

Hwang, S. W., Chung, H., Lee, T., Ahn, K. S., Pang, S. J., Bang, J., Kwak, H. W., Oh, J. K., and Yeo, H. (2022). "Monitoring of moisture and dimensional behaviors of nail-laminated timber (NLT)-concrete slab exposed to outdoor air," *Journal of the Korean Wood Science and Technology* 50(5), 301-314. DOI: 10.5658/WOOD.2022.50.5.301

Hwang, S. W., Hwang, S. Y., Lee, T., Ahn, K. S., Pang, S. J., Park, J., Oh, J. K., Kwak, H. W., and Yeo, H. (2021). "Investigation of electrical characteristics using various electrodes for evaluating the moisture content in wood," *BioResources* 16(4), 7040-7055. DOI: 10.15376/biores.16.4.7040-7055

Kaleta-Jurowska, A., and Jurowski, K. (2020). "The influence of ambient temperature on high performance concrete properties," *Materials* 13(20), article 4646. DOI: 10.3390/ma13204646

Kim, J. H., and Lee, W. H. (2002). "Physical properties of larch (*Larix kaempferi* Carr.) treated by high temperature steaming - Effect of high temperature steaming on shrinkages of larch block," *Journal of the Korean Wood Science and Technology* 30(2), 102-107.

Kirker, G. T., Bishell, A. B., and Zelinka, S. L. (2016). "Electrical properties of wood colonized by *Gloeophyllum trabeum*," *International Biodeterioration & Biodegradation* 114, 110-115. DOI: 10.3390/ma13204646

Liang, S., Gu, H., Bergman, R., and Kelley, S. S. (2020). "Comparative life-cycle assessment of a mass timber building and concrete alternative," *Wood and Fiber Science* 52(2), 217-229.

Lin, F., and Meyer, C. (2009). "Hydration kinetics modeling of Portland cement considering the effects of curing temperature and applied pressure," *Cement and Concrete Research* 39(4), 255-265. DOI: 10.1016/j.cemconres.2009.01.014

Lukaszewska, E., Johnsson, H., and Fragiacomo, M. (2008). "Performance of connections for prefabricated timber–concrete composite floors," *Materials and Structures* 41, 1533-1550. DOI: 10.1617/s11527-007-9346-6

Ng, P. L., and Kwan, A. K. (2016). "Strategies for improving dimensional stability of concrete," *Canadian Journal of Civil Engineering* 43(10), 875-885. DOI: 10.1139/cjce-2016-009

Ou, Y., Gattas, J. M., Fernando, D., and Torero, J. L. (2020). "Experimental investigation of a timber-concrete floor panel system with a hybrid glass fibre reinforced polymer-timber corrugated core," *Engineering Structures* 203, article 109832. DOI: 10.1016/j.engstruct.2019.109832

Pang, S. J., Ahn, K. S., Kim, M. J., Hwang, S. W., Kang, S. G., Kwak, H. W., Yeo, H., and Oh, J. K. (2022). "Effect of intumescent coating on the charring rate of nail-laminated Timber," *BioResources* 17(4), 5999-6018. DOI: 10.15376/biores.17.4.5999-6018

Park, Y., Han, Y., Park, J. H., Chang, Y. S., Yang, S. Y., Chung, H., Kim, K., and Yeo, H. (2015). "Evaluation of physico-mechanical properties and durability of *Larix kaempferi* wood heat-treated by hot air," *Journal of the Korean Wood Science and Technology* 43(3), 334-343.

Pierobon, F., Huang, M., Simonen, K., and Ganguly, I. (2019). "Environmental benefits of using hybrid CLT structure in midrise non-residential construction: An LCA based comparative case study in the US Pacific Northwest," *Journal of Building Engineering* 26, article ID 100862. DOI: 10.1016/j.jobe.2019.100862

Sakata, K. (1983). "A study on moisture diffusion in drying and drying shrinkage of concrete," *Cement and Concrete Research* 13(2), 216-224. DOI: 10.1016/0008-8846(83)90104-7

Shupe, T., Lebow, S., and Ring, D. (2008). *Causes and Control of Wood Decay, Degradation & Stain*, Louisiana State University Agricultural Center, Baton Rouge, LA, USA.

Sinha, A., Udele, K. E., Cappellazzi, J., and Morrell, J. J. (2020). "A method to characterize biological degradation of mass timber connections," *Wood and Fiber Science* 52(4), 419-430.

Yeoh, D. (2010). *Behaviour and Design of Timber-Concrete Composite Floor System,* Doctoral Thesis, University of Canterbury, Christchurch, New Zealand.

Yeoh, D., Fragiacomo, M., De Franceschi, M., and Heng Boon, K. (2011). "State of the art on timber-concrete composite structures: Literature review," *Journal of Structural Engineering* 137(10), 1085-1095. DOI: 1943-541X.0000353